



---

**Status report on the WP2 of the  
Swiss-Danish instrumentation work packages  
for the European Spallation Source, ESS**

**focusing reflectometer (Selene)**

---

---

J. Stahn, November 15, 2012



Paul Scherrer Institut



---

Switzerland	PSI	Jochen Stahn Panagiotis Korelis Uwe Filges Tobias Panzner
Denmark	CU	Marité Cardenas Ursula Hansen
	USD	Beate Klösgen

---

## project team

Jochen Stahn senior scientist  
Laboratory for Neutron Scattering  
Paul Scherrer Institut  
Switzerland  
jochen.stahn@psi.ch  
+41 56 310 2518

Panagiotis Korelis pst-doc  
Laboratory for Neutron Scattering  
Paul Scherrer Institut  
Switzerland  
panagiotis.korelis@psi.ch  
+41 56 310 5813

Uwe Filges senior scientist  
Laboratory for Developments and Methods  
Paul Scherrer Institut  
Switzerland  
uwe.filges@psi.ch  
+41 56 310 4606

Tobias Panzner pst-doc  
Laboratory for Developments and Methods  
Paul Scherrer Institut  
Switzerland  
tobias.panzner@psi.ch  
+41 56 310 4342

Marité Cardenas senior scientist  
Nano-Science Center  
University of Copenhagen  
cardenas@nano.ku.dk  
+45 35 320 431

Ursula Bengaard Hansen student assistant  
Nano-Science Center  
University of Copenhagen  
uhansen@fys.ku.dk  
+45 60 478 615 (mobile)

Beate Klösgen associate professor  
MEMPHYS, Department for Physics, Chemistry and Pharmacy  
University of Southern Denmark  
Denmark  
kloesgen@sdu.dk  
+45 6550 2561

*Selene*



titan goddess  
moon, dark side

detail of the ceiling painting  
*Selene and Endymion*  
at the  
*Ny Carlsberg Glyptotek, Copenhagen*

# Contents

<b>introduction</b>	<b>4</b>
<b>1 prototype</b>	<b>5</b>
1.1 design considerations . . . . .	5
1.2 devices . . . . .	5
1.2.1 pulse chopper . . . . .	5
1.2.2 frame-overlap chopper . . . . .	5
1.2.3 precision slit . . . . .	6
1.2.4 double multilayer monochromator . . . . .	6
1.2.5 sample holder . . . . .	6
1.2.6 guide support . . . . .	6
1.2.7 guide system . . . . .	7
1.3 experiments on BOA . . . . .	9
1.3.1 BOA . . . . .	9
1.3.2 set-up . . . . .	9
1.3.3 experiments in TOF mode . . . . .	10
1.3.4 experiments with angle-wavelength encoding . . . . .	12
1.3.5 use of a diffusor . . . . .	12
1.3.6 discussion . . . . .	13
1.4 experiments on Amor . . . . .	15
1.4.1 Amor . . . . .	15
<b>2 reflectometer for tiny samples</b>	<b>16</b>
2.1 science case . . . . .	17
2.2 single-Selene guide system . . . . .	19
2.3 double-Selene guide system . . . . .	23
<b>3 reflectometer with a horizontal sample surface</b>	<b>26</b>
3.1 science case . . . . .	26
3.2 instrument . . . . .	26
3.2.1 operation principle . . . . .	26
3.2.2 McStas simulations . . . . .	29
<b>A publications</b>	<b>30</b>

## introduction

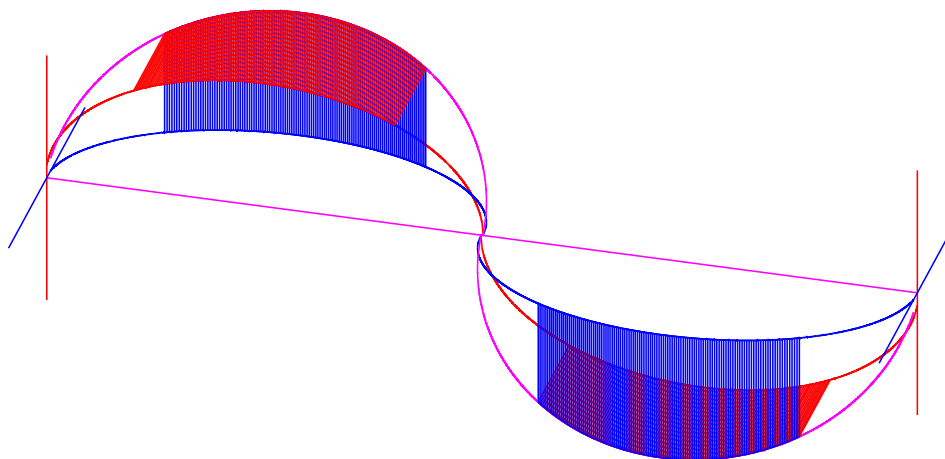
The *Swiss-Danish Instrument Initiative* proposes to build several, but highly optimised instruments of one class, rather than one flexible instrument with moderate performance due to the necessary compromises. As “guiding ideas” we suggest I a small sample size, II a horizontal sample interface, and eventually III high resolution in  $q_y$  (i.e. GISANS).

Optimisation requirements of I and II exclude each other to some extent: The vertical scattering plane imposes quite severe constraints for high-angle diffraction, and gravitation effects become important. On the other side typical samples with liquid/liquid or liquid/gas interfaces are larger than  $10 \times 10 \text{ mm}^2$ , while really *small* samples are the order  $100 \times 100 \mu\text{m}^2$ .

A generic reflectometer is designed on the basis of using elliptically shaped guides and focusing to the sample in both directions normal to the beam (section ??).

The usage of point-to-point focusing rather than a straight guide leads to a drastically reduced beam intensity in the guide, while almost conserving the phase space density actually needed for the measurements. Also the beam is convergent at the sample which avoids over-illumination of the sample (if required) and of the sample environment.

The idealised set-up consists of two subsequent identical guides (see sketch below and figure ??). Each guide has one reflecting surface shaped like one branch of an ellipse for each direction (like a Montel optics as used at synchrotron beam line).



The (virtual) source is mapped by the first guide to an intermediate image, which is then mapped to the sample position. This way the coma aberration inherent to elliptic reflectors is almost completely corrected for. The maximum divergence  $\Delta\theta$  is given by the acceptance of the first ellipse. It can be reduced by an aperture in between the focal planes. The spot-size at the sample position is (almost) identical to the source size, i.e. it can be adjusted by slits at the first focal point without changing  $\Delta\theta$ .

With reference to the half-elliptical shape of the light-to-shadow border on the moon we call this the *Selene* set-up.

In the following sections the generic lay-out of the instrument is presented, followed by discussions of its components from source to detector. Based on these considerations two possible realisations for the ESS are presented, one optimised for small samples (with horizontal scattering plane, section 2) and one optimised for liquid interfaces (section 3). The design and realisation of a prototype *Selene* guide is presented in section 1.

# 1 prototype

## 1.1 design considerations

The prototype was designed to operate in a  $\lambda$ - and  $\theta$ -range close to what can be expected for a reflectometer at the ESS, paying respect to the beam characteristics and spacial constraints at BOA (1.3.1) and Amor (1.4.1).

- length of the focusing section ( $= 4c$ ): The available space at BOA is some 9 m. About 3 m are needed to get an acceptable angular resolution on the detector ( $\Delta\theta \approx 0.04^\circ$ ). Another 1.5 m before the first focal point are required for the ml-monochromator, the chopper and eventually further equipment. This led to  $4c = 4$  m.
- divergence: The divergence was chosen to be slightly larger than what is available at BOA or Amor, i.e.  $\Delta\theta = 1.8^\circ$ .
- ellipse parameters: The effective length was defined to  $\xi = 0.60$ , leading to  $b/a = 0.021480$ .
- $\lambda$ -range: The  $\lambda$ -range was selected based on the considerations made in (??) to be  $\lambda \in [3.8, 12]$  Å. This results in a coating with  $m = 4$ .
- sample size: For  $c = 1$  m and the typical  $b/a \approx 0.02$  the maximum spot size with only small influence of coma aberration is  $1 \times 1$  mm<sup>2</sup>. Larger spots are possible, but the footprint the is no longer homogeneous.
- chopper speed and pulse length: To cover the required  $\lambda$ -range in time-of-flight with a possible chopper-detector distance of some 8 m one needs a frequency of  $\approx 60$  s<sup>-1</sup>. The chopper opening-to closing time ratio is the same as for the ESS pulses, i.e. 0.04.

## 1.2 devices

Most of the following devices were designed, constructed and fabricated at PSI. The exceptions are the X95 elements, the precision slit and the guide elements.

### 1.2.1 pulse chopper

The reduced length of the set-up compared to the ESS dimensions with about the same  $\lambda$  range leads to shorter repetition rate and pulse length for the test set-up. The pulse chopper will operates with up to 60 Hz, its open/closed time ratio is about 5% (to be determined exactly). The chopper disc has 2 openings.

The much reduced dimension of the beam relative to conventional set-ups leads to a disc diameter of  $\varnothing = 160$  mm. The absorbing material is 2.2 mm of an Al :<sup>10</sup>B alloy, followed by 2 mm Cd. The absorbing region is 10 mm wide. Figure 1 shows on the left side the pulse chopper after assembling, before testing.

The pulse chopper is equipped with a !!! to trigger the TOF data acquisition. Since this system detects each gap opening of the chopper, no correction for the second gap and eventually an phase error is needed.

### 1.2.2 frame-overlap chopper

The frame overlap chopper has similar dimensions as the pulse chopper, but a open/close time ratio of 50%. Its position is at or close to the intermediate focal point of the *Selene* guide system. The frequencies and phases of pulse- and frame-overlap-choppers can be locked. The frame overlap chopper is the left device in figure 1.

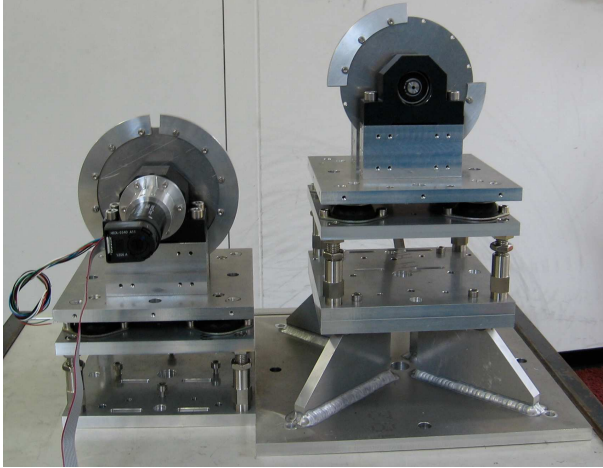


Figure 1: Pulse chopper (left) and frame overlap chopper (right) for the *Selene* prototype.

### 1.2.3 precision slit

The small dimensions of the prototype results in a down-scaling of the sample and thus of the slit at the first focal point. The beam cross section is of the order  $0.1 \times 1 \text{ mm}^2$ . This will be realised with a precision x-ray slit system, equipped with BorAl and Cd absorbers. The slit is custom made by ACS and based on their system STT-100-20.

During the experiments on BOA the slit failed several times. In the end it could not be used other than for defining a fix opening of approximately  $0.5 \times 1 \text{ mm}^2$ .

### 1.2.4 double multilayer monochromator

The double multilayer monochromator consists of 2 borcron glass substrates, coated with a Ni/Ti multilayer with a first order peak at  $m = 3$  with  $\Delta q/q = 7\%$ . The surfaces are mounted parallel face to face with a gap of 6.5 mm. The first substrate is 305 mm long, the second 119 mm. In  $x$  direction there is a 5 mm gap in between both. The design is optimised for a slit positioned 43 mm behind the end of the device. The acceptance is  $\Delta\theta = 1.8^\circ$  for  $\lambda \in [4, 10] \text{ \AA}$ .

The device was tested and characterised on Amor. Since the divergence available for this test was only of the order of  $0.3^\circ$ , the full angular range was reached by tilting the monochromator in discrete steps. Figure 2 shows the resulting  $I(\theta, \lambda)$  map. The width of the intensity streak shown here is limited by the measurement range, not by the device.

To characterise  $\Delta\lambda/\lambda$  and the off-specular scattering, also measurements were performed with a well collimated beam (slits of 1 mm opening, 100 mm and 2200 mm from the entrance of the device). The  $I(\lambda)$  curves for various  $\theta$  is shown in figure 3.

Figure 4 shows the off-specular scattering for  $\lambda = 6.3 \text{ \AA}$  with various slit positions and openings behind the device. The slits before the ml-monochromator are 1 mm each. Surprisingly there is the same broad diffuse background with an exponential decay for all measurements. The origin is unclear yet, but eventually this is a feature of the detector.

### 1.2.5 sample holder

The sample holder is simply an Al cuboid with grooves and slits to insert (glue) the sample and some absorbing sheets. It is mounted on a  $y$  and  $z$  translation stage.

### 1.2.6 guide support

The guide support system is assembled from X95 profiles and joints, motorised and manual translation tables and manual tilting stages. Figure 5 shows the mounting frames for the single guide elements (figure 7), the height and tilt-adjustments and the X95 bar where upon the guide elements are mounted. This bar is positioned on tilting- and translation stages, which are to be mounted to the lower rotation stages of the BOA tables 3 and 4, respectively.

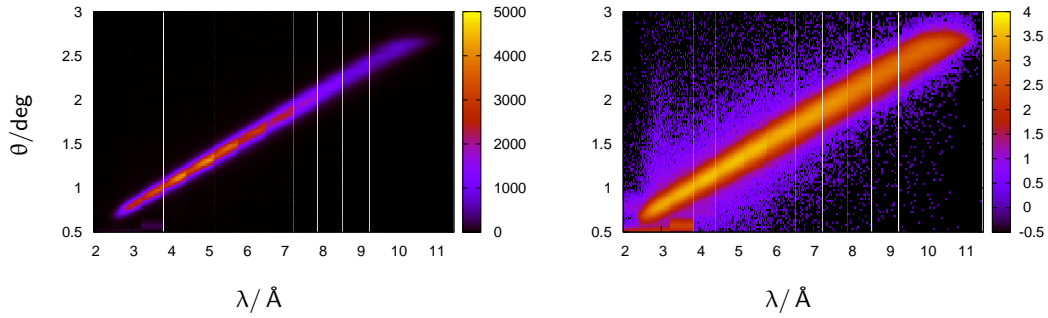


Figure 2:  $I(\lambda, \theta)$  on linear (left) and logarithmic scale (right) obtained with the ml-monochromator on Amor. The maps are stitched together from 11 measurements since the incoming divergence was limited to  $0.3^\circ$ .

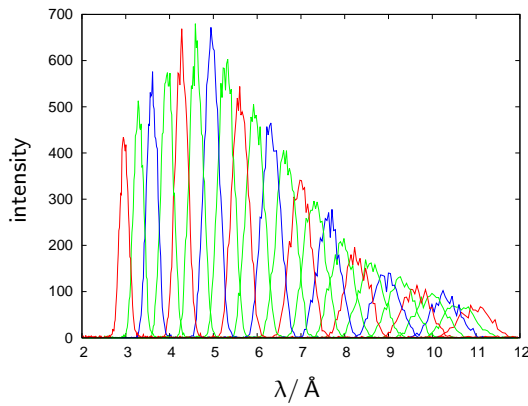


Figure 3:  $I(\lambda)$  for  $\theta = 0.5^\circ, 0.6^\circ, \dots, 3.0^\circ$ . The varying height of the individual scans reflects the  $\lambda$ -dependence of the intensity of the incoming beam.

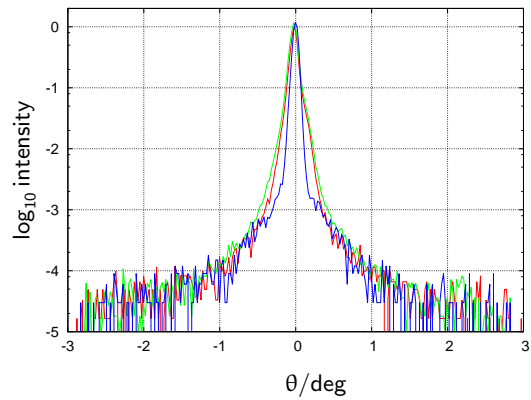


Figure 4:  $\log_{10}[I(\theta)]$  without aperture behind the device (green), with a 0.5 mm aperture at 50 mm (red), and with a 1 mm aperture at 1300 mm (blue).

### 1.2.7 guide system

The *Selene* guide system in this case consists of 2 sections focusing elliptically in two dimensions (i.e. in  $y$  and in  $z$ ), where each section consists of 2 mirror-inverted elements of 600 mm length. Figure 7 shows one guide element before mounting.

The device was constructed and built by SwissNeutronics according to the measures  $c = 1000$  mm,  $b/a = 0.021480$ ,  $\xi = 0.60$ , coating Ni/Ti with  $m = 4$ . The horizontally reflecting glass substrate has a constant height of 46 mm. The vertically reflecting glass has one straight edge along the optical axis, and one elliptically curved edge, fitting the horizontal reflectors shape. The vertical reflector has a minimum width of 21 mm.



Figure 5: Parts of the guide support before mounting the guide elements.

Figure 6: Guide support with 2 guide elements mounted. Shown is the second guide of the *Selene* set-up, reflecting left and downwards. The guides are not yet adjusted, the knife blade slit is missing.



Figure 7: Single guide element (half a guide section). The blue part is an L-shaped Al bar on which the glass substrates are screwed. The Al frames are for mounting the elements on the support and alignment system.

## 1.3 experiments on BOA

The *Selene* prototype was first set up and tested on the beamline BOA at SINQ, PSI, in August and September 2012. The team members for this campaign were U. B. Hansen, T. Panzner, and J. Stahn.

The intensity available at BOA together with the high background limited strongly what could be measured. Since both, chopper and ML-monochromator have a transmission of ca. 5%, only, it was not possible to operate them simultaneously for TOF  $\lambda$ - $\theta$ -encoding.

In the meantime (11. 2012) the background could be reduced by almost 2 orders of magnitude, so further tests on BOA are scheduled for December 2012 and for 2013.

### 1.3.1 BOA

(by U. Filges)

BOA stands for "beam line for neutron optics and other applications" and is operated by the Neutron Optics group within the Laboratory for Development and Methods at PSI. [U. Filges, Swiss Neutron News, **40**, 4 (2012)] The beam line is a 18 m long instrument located at beam-channel 51 looking at the SINQ cold source which delivers a neutron spectrum from 1.5 Å to 20 Å. The guide section contains a supermirror bender unit inside the SINQ biological shielding. Thus the beam is permanently polarised in vertical direction.

The flexible space is 12.5 m long (n-flight path) and 3.5 m wide. Where the first part is occupied by an anti-trumped within a concrete shielding. The instrument is equipped with 5 x-translation tables on an optical bench, where the 3 latter are motorised and hold each a y-translation stage. On these platforms optional  $\omega$  and  $2\theta$  rotation stages, goniometers, and further translation stages can be mounted. An area sensitive CCD camera system, a  $^3\text{He}$  neutron counter system, and a  $^3\text{He}$  area detector (EMBL) are used for data acquisition. Figure 8 shows the essential components of the beamline with the *Selene* prototype set-up in place.

### 1.3.2 set-up

All components were mechanically ready by mid August 2012. The installation on BOA started on 13. August. In parallel the motorised components were commissioned and integrated into the instrument control system (translation devices, slit system) or operated as stand-alone solutions (choppers).

First the complete set-up was realised using the instruments LASER for the mean beam direction and the instruments light source giving a white divergent light to align the guide elements. *Figure of merit* at the

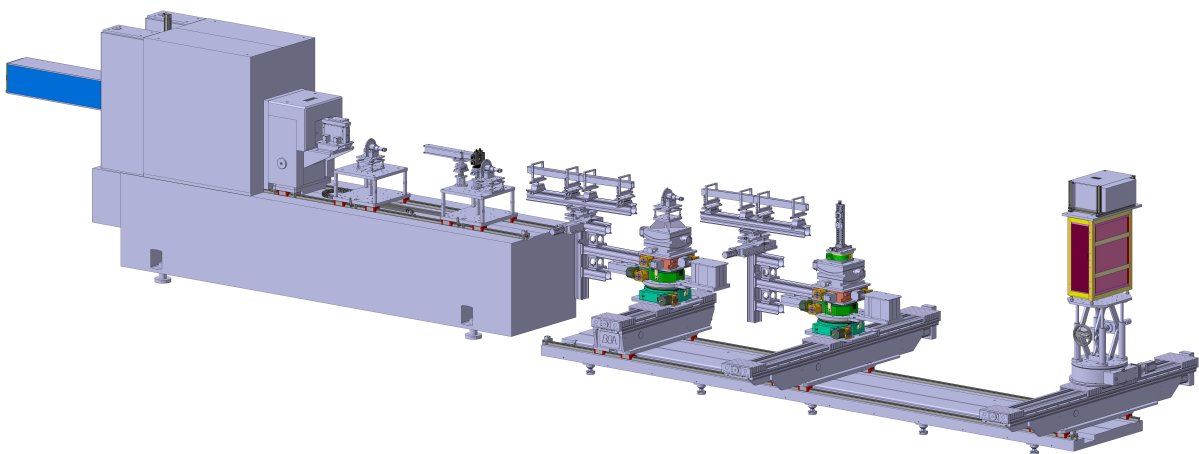


Figure 8: Assembly drawing of the construction of the *Selene* prototype set-up on the test facility BOA at PSI. The elements/devices from left to right: n-guide of BOA; pulse chopper on table 2; double ml monochromator, precision slit, pulse chopper (alternative position) on table 3; first guide section on support system, attached to table 4; frame overlap chopper on table 4; second guide section on support system, attached to table 5; sample holder on yz translation stage on table 5; and area detector on table 6.

beginning was to achieve a symmetric, small light spot at the focal points, and a homogeneous, gap-free light distribution on the detector. The first requirement could be fulfilled rather easily (the spot at the sample position is almost identical to the one defined by a pin-hole). The second task proved to be more complicated since the light source produced a highly structured beam, covering mis-alignments. Thus in a later stage a high-power LED with a reflector (bicycle front light) was used in front of the pin-hole.

### 1.3.3 experiments in TOF mode

The choppers were operated at  $1800 \text{ min}^{-1}$ , i.e. with a pulse rate of  $60 \text{ s}^{-1}$ . The phase of the frame-overlap chopper was chosen to select  $\lambda \in [2, 13] \text{ \AA}$ .

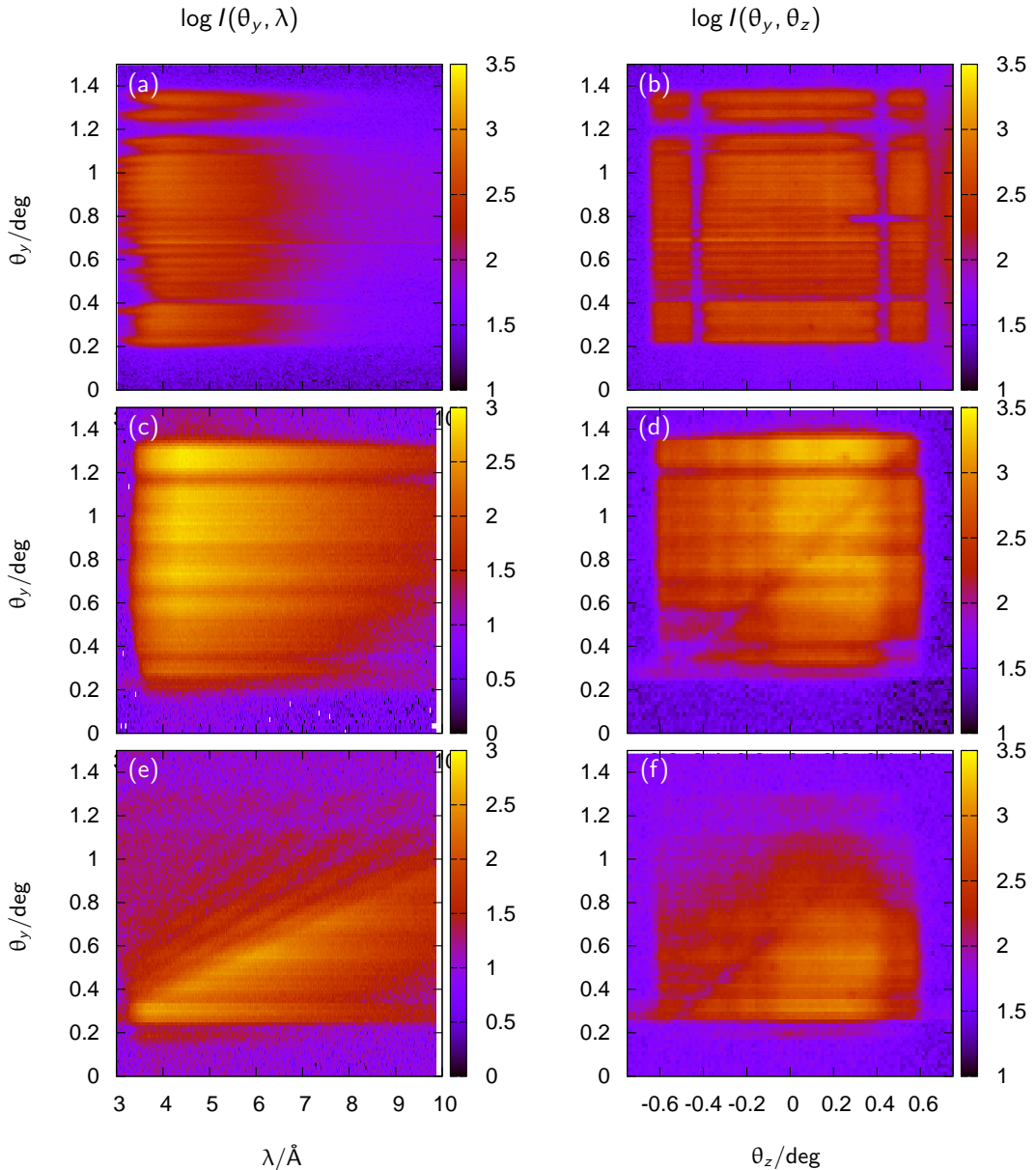


Figure 9: Intensity maps  $\log I(\theta_y, \lambda)$  and  $\log I(\theta_y, \theta_z)$  for the beam emerging from the precision slit (a) and (b), after the *Selene* guide being reflected by a  $m = 5$  Ni/Ti supermirror (c) and (d), and being reflected by a  $1000 \text{ \AA}$  thick Ni film on glass (e) and (f).

## characterisation of the beam

The beam characteristics behind the precision slit was measured with the area detector 5100 mm behind the slit in TOF mode. Due to the bender section in the BOA neutron guide the divergence is strongly patterned in horizontal direction. Reflections on sidewalls (anti-trumpet) and on roof and bottom lead to the higher divergence contributions. In between there is a low-intensity gap. Figure 9 (a) and (b) shows the intensity maps  $I(\theta_y, \lambda)$  and  $I(\theta_y, \theta_z)$ , obtained from the TOF data by integrating horizontally, or over time. The dark horizontal area in (b) on the right side results from a mechanical damage in the bender section. The horizontal high intensity streak at  $\theta_y \approx 0.7^\circ$  is a feature of the area detector.

Map (a) shows the strong  $\lambda$  dependence of the primary intensity. The  $I(\lambda)$  depends also on where the individual channels of the bender point towards the moderator.

The large dynamic range of  $I(\lambda)$  here is attenuated by the 4 reflections in the *Selene* guide, which mainly affect short wavelengths.

## reflection of a $m = 5$ supermirror

For normalisation of the beam reflected off a sample, a similar measurement using a supermirror can be used. Available are such references with a Ni/Ti supermirror coating of  $m = 5$  with area  $1 \times 2 \text{ mm}^2$ ,  $3 \times 3 \text{ mm}^2$ , and  $10 \times 10 \text{ mm}^2$ .

Figures 9 (c) and (d) show intensity maps similar to the ones mentioned above, but this time measured using the *Selene*-guide. The sample was the  $10 \times 10 \text{ mm}^2$  SM, the beam size was 1 mm high and 0.5 mm wide. This means that the sample was illuminated completely along the neutron beam direction. The diagonal dark streak visible in figure 9 (d) originates from the areas of the *Selene* guide elements where the horizontal and the vertical reflector join. Tiny errors in the surface quality and the shape of the substrates (caused by the cutting process) leads to a lower reflectivity there. This is inherent to the Montel-type optics. For larger guide systems this feature will be much weaker since the absolute width of the distorted area stays the same, while the guide dimensions get much larger.

The stripe pattern visible in both maps has several origins: besides the inhomogeneities imposed by the beam characteristics of BOA, there are imperfections of the guides (waviness) and more severe, inhomogeneities of the area detector.

The low-intensity region in 9 (d) in the lower left corner is a feature of the *Selene* optics: the coma aberration is corrected for in space, but in momentum space some inhomogeneities remain.

## reflection of a 1000 Å thick Ni film on glass

As a sample the reference for characterising and adjusting the TOF reflectometer Amor was used: a 1000 Å thick Ni film on glass. Figures 9 (e) and (f) show the corresponding intensity maps. The *triangle* below the diagonal in map (e) is caused by total reflection off the Ni film. Thus it looks similar to the same region in map (c). The fan-like structure corresponds to the Kiessig fringes. Each horizontal line can be seen as a TOF measurement of a range of the reflectivity curve, where  $\theta_y$  acts as a scaling factor. But also each vertical line represents a reflectivity measurement, this time in angle-dispersive mode for a given  $\lambda$ .

To obtain a reflectivity curve, the intensity map from the sample has to be divided pixel-by-pixel by the reference measurement (here with the SM). The result is shown in figure 10 (a). Then  $I(\theta_y, \lambda)$  is transferred to  $I(\theta_y, q_z)$  on an (here) equidistant  $q_z$  grid to give map (b). Then each horizontal line is normalised so that the total reflection plateau is at  $I = 1$ . The horizontal stripes still visible in map (c) have 2 origins: e.g. the prominent line at  $\theta_y \approx 1.2^\circ$  results from the division of noise by noise in the angular region where (nearly) no intensity is available. The sharper lines result from inhomogeneities of the detector. The maps have not been measured on exactly the same area of the detector, but were shifted by some pixels. Thus the normalisation did not correct for different efficiencies of the detector.

The reflectivity curve in Figure 10 (d) was obtained by a wighted summation over the  $\theta_y$ -channels. No error-handling was applied so far with the consequence that the noise from the region  $\theta_y \approx 1.2^\circ$  dominates the curve at high  $q_z$ . In this graph only 5 Kiessig fringes are clearly visible, while in the maps on can count 7. This means a more accurate data analysis will provide a better  $R(q_z)$  curve. But still the background sets a limits at about  $10^{-3}$ . This is why the experiment is going to be repeated on the TOF reflectometer Amor, which reaches  $10^{-5}$  for small samples ( $5 \times 5 \text{ mm}^2$ ) in a reasonable time in *normal* operation.

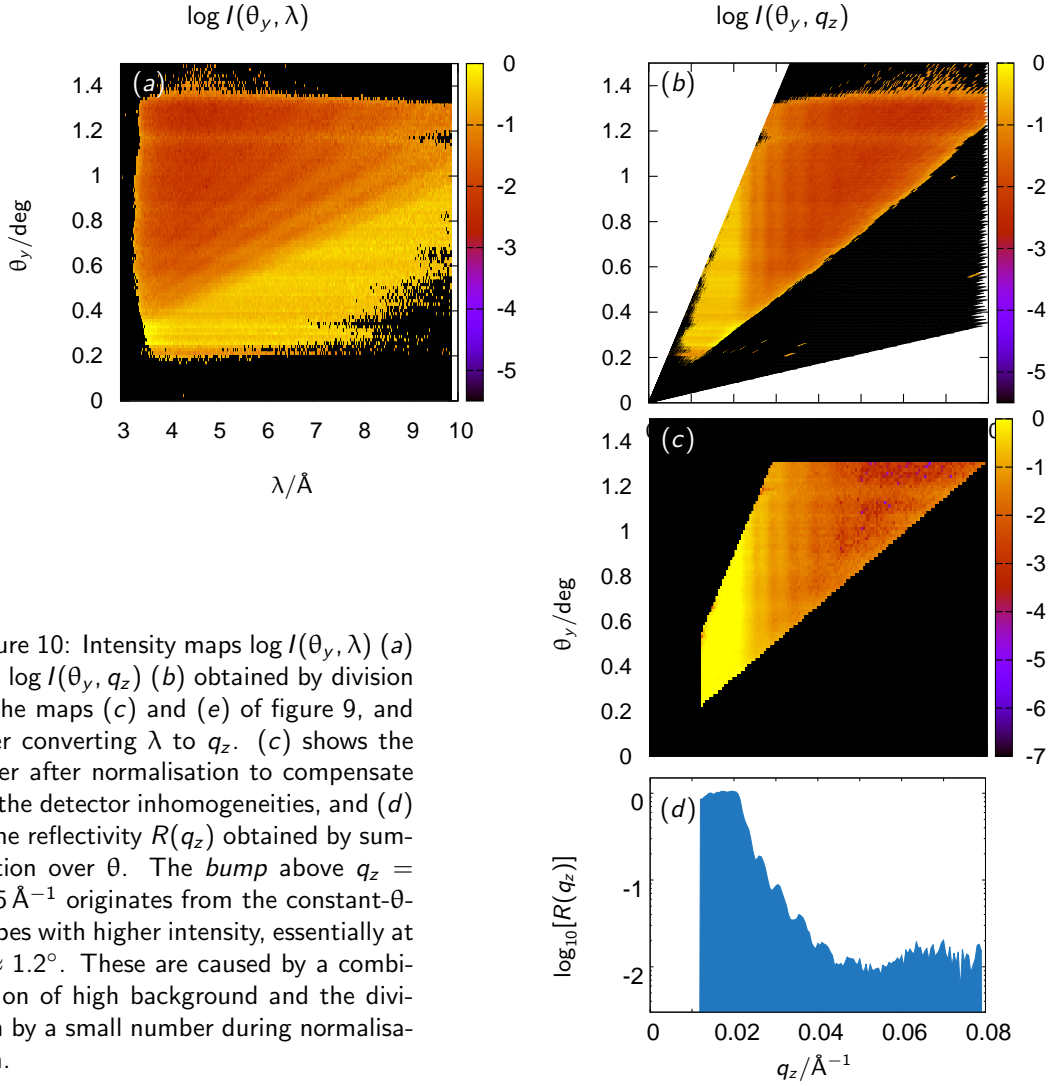


Figure 10: Intensity maps  $\log I(\theta_y, \lambda)$  (a) and  $\log I(\theta_y, q_z)$  (b) obtained by division of the maps (c) and (e) of figure 9, and after converting  $\lambda$  to  $q_z$ . (c) shows the latter after normalisation to compensate for the detector inhomogeneities, and (d) is the reflectivity  $R(q_z)$  obtained by summation over  $\theta$ . The *bump* above  $q_z = 0.05 \text{\AA}^{-1}$  originates from the constant- $\theta$ -stripes with higher intensity, essentially at  $\theta \approx 1.2^\circ$ . These are caused by a combination of high background and the division by a small number during normalisation.

### 1.3.4 experiments with angle-wavelength encoding

For these measurements the chopper was stopped (in the open position), and the double ML-monochromator was installed before the precision slit. Measurements analogue to the ones discussed in 1.3.3 were performed. But in this case the inhomogeneities of the detector prevent the calculation of  $R(q_z)$ , thus a repetition is planned where it is made sure that both maps, from the sample and from the reference, are collected on exactly the same area on the detector.

#### reflection of a $m = 5$ supermirror

data analysis not completed

#### reflection of a $1000 \text{\AA}$ thick Ni film on glass

data analysis not completed

### 1.3.5 use of a diffusor

One can use the *Selene* guide to create a small virtual source far from the moderator. This might be of interest e.g. for an imaging beam line. In this case the beam emerging from the last focal point should have a homogeneous  $I(\theta_x, \theta_y)$  distribution. Since in the present case the source is inhomogeneous (see figure 9 (b))

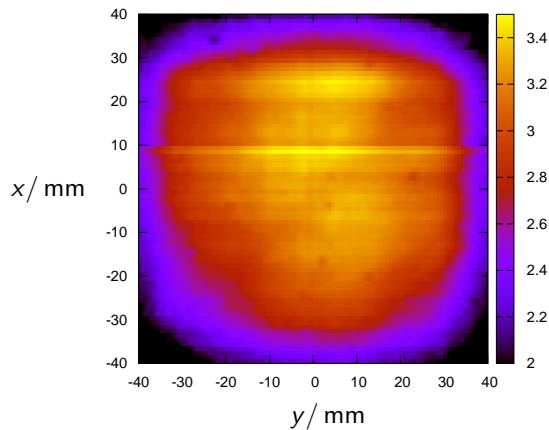


Figure 11: Intensity map  $I(x, y)$  measured in direct view to the *Selene* guide with a 2 mm thick graphite plate at the sample position, acting as a diffusor. The distance from the graphite to the detector was 3200 mm. The bright horizontal stripe at  $x \approx 9$  mm originates from a defect of the detector (electronics?).

also the divergence after the *Selene* guide is. For the intensity map shown in figure 11 a 2 mm thick graphite plate was positioned at the focal point instead of the sample.

data analysis not completed

### 1.3.6 discussion

The intended program for the first beamtime on BOA was too ambitious. Instead of the measurement of  $R(q_z)$  of a reference sample in all principle operation modes (with chopper, with ML monochromator, using both), only the chopper mode was at least partly completed.

The main problems are not connected to the *Selene* guide but result from the experimental environment and the equipment:

- High background caused by fast neutrons coming down the guide, and by thermal neutrons from the neighbouring imaging beamline ICON.
- In the meantime the background could be lowered by 2 orders of magnitude. The improvements on shielding are based on the measurements within this campaign.
- Inhomogeneous sensitivity of the  $^3\text{He}$  area detector.
- Inhomogeneous beam profile and divergence of the beam leaving the BOA guide.
- This can be reduced by installing a graphite diffusor before the initial slit.
- Surprisingly low intensity.

On the other side it proved to be quite simple to align the guide elements using a (homogeneous) white light source before the initial focal point.

### guide quality

The overall quality of the guide is very good. Compared to the first elliptically focusing guide produced for Amor there is a huge progress made by SwissNeutronics.

- Still there is some waviness visible, where the *propagation of the waves* is parallel to the neutron beam direction.

- The effect is so small that it hardly affects the data analysis.
- The two substrates for the horizontal and the vertical reflecting part of one guide element do not form exactly a  $90^\circ$  angle.
- This prohibits a simultaneous perfect alignment of the guide elements in both directions. An improvement is possible.
- At the region where two elements join the reflectors do not exactly follow an elliptic shape, leading to a reduced intensity coming from there.
- This should be improved. Off-situ analysis using light is planned to identify the real shape.

### **measurements**

- For the chopper-only mode the inhomogeneities mentioned above play a minor role. Essentially they just lead to a reduction of the intensity. So in this case the measurements have been successful in a sense that a reflectivity curve could be measured. Limitations were imposed by the long counting time and the high background limiting the dynamic range.
- Using both, chopper and ML-monochromator was not successful: The much too low intensity even prohibited to align the sample.
- The data obtained with a ML-monochromator only, are not yet analysed completely. But since there the inhomogeneities of the beam and the detector directly influence the resolution and the  $\lambda$ - $\theta$  encoding, it will be no surprise if the data analysis fails.

### **outlook**

Further tests of the *Selene* prototype are planned on Amor beginning of November, and on BOA beginning of December. Amor offers a much lower background and should allow for a simultaneous use of choppers and ML-monochromator.

SwissNeutronics will improve the alignment of the reflectors within one guide element.

## 1.4 experiments on Amor

### 1.4.1 Amor

Amor is a neutron reflectometer which allows for a wide range of set-ups. The scattering geometry is vertical so that liquid surfaces are accessible. Most components are positioned on an optical bench which allows to play with the resolution, or to test exotic set-ups like the prism approach by R. Cubitt [?] or the *Selene* concept. In general Amor is operated in time-of-flight mode (realised by a double chopper), but it is also possible to run it with a monochromator.

Figure ?? shows a sketch of Amor in the scattering plane with the *Selene* set-up realised (monochromatic and TOF mode). For the tests presented here, ...

The ML-monochromator is placed on the frame-overlap mirror stage and can be driven out of the beam.

The chopper is positioned in a housing, some cm behind the end of the neutron guide. It consists of 2 discs, 490 mm apart, each with 2 openings of  $13.6^\circ$ . In general it is operated in a way to give  $\Delta\lambda/\lambda = \text{const.}$ [?]

The chopper housing limits the maximum incoming divergence because it leads to a minimum distance between the end of the guide to the first diaphragm of 1500 mm, and to the first place where to put a monochromator (on the frame overlap filter stage) it is some 1800 mm.

For the tests we used a pulse frequency of  $23.\bar{3}$  Hz (corresponding to 700 rpm).

Behind the chopper housing and the 1<sup>st</sup> diaphragm a frame overlap filter is mounted. It consists of Si-wafers of 0.6 mm thickness, coated with a Ni/Ti  $m^f = 2$  SM. If placed in the beam with an inclination of  $\theta^f$  it reflects all neutrons with  $\lambda > 4\pi \sin \theta^f / m^f q_{\text{Ni}}^c$ .

In the case of the strongly divergent beam the deviation of  $\alpha^f$  from  $\theta^f$  has to be taken into account. The cut-off wavelength is then  $\lambda^f = 4\pi \sin(\theta^f - \theta) / m^f q_{\text{Ni}}^c$ .

In TOF mode (without monochromator) the situation is more complicated: All neutrons accepted by the elliptic guide should have all required wavelengths. But the flat filter acts angle dependent! A possible solution is to build an logarithmically bent filter. This then is optimised for one specific cut-off wavelength.

fixed values	/	mm
guide end – chopper housing start	:	75
guide end – chopper housing end	:	1309
guide end – 1 <sup>st</sup> chopper disc	:	?
guide end – earliest position polariser	:	2744
guide end – lead aperture	:	?
1 <sup>st</sup> slit – earliest position polariser	:	1242
5 <sup>th</sup> slit – single detector	:	?
typical values		
chopper disc 1 – chopper disc 2	:	490
1 <sup>st</sup> slit – 2 <sup>nd</sup> slit	:	?
2 <sup>nd</sup> slit – 3 <sup>rd</sup> slit	:	?
3 <sup>rd</sup> slit – sample	:	400
sample – 4 <sup>th</sup> slit	:	400
sample – single detector	:	?

Table 1: List of typical or fixed distances on Amor.

## 2 reflectometer for tiny samples

The leading design task for this instrument is to be able to perform reflectometry on *small samples*. I.e. the flux and the pulse structure of the ESS are mainly used to achieve this goal. Other tasks as high  $q_z$  range, time resolved measurements, polarisation, ... are still possible. The instruments optimisation towards them just should not affect (severely) the leading task. *Small* here means surface area one or 2 orders of magnitude smaller than presently possible (as a standard method).

We aim for a footprint size from  $10 \times 10 \text{ mm}^2$  (state-of-the-art) down to  $0.3 \times 0.3 \text{ mm}^2$ . This is optimal for samples who's (homogeneous) size is restricted by the preparation method to below  $1 \text{ cm}^2$ , e.g. PLD-grown metal-oxide heterostructures. Due to the wide variety of properties they offer based on composition (like ferro- or antiferromagnetism, superconductivity, isolation, conductance, multiferroicity, etc.) they form a large and rapidly growing field in material science. Bent or curved surfaces become accessible because the beam footprint can be restricted to a small area and thus the angular resolution is hardly affected. Inhomogeneous samples can be scanned, e.g. to avoid areas with damages, non-perfect coating, or gas bubbles in liquid/solid cells.

The instrument is flexible enough to measure all kinds of samples besides liquid/liquid or liquid/gas interfaces. The wide free space around the sample position allows for bulky sample environment, and for simultaneous usage of complementary techniques.

The Selene guide concept combines the two conventional reflectometer types using angular or time-of-flight resolution. The resulting time-dependent phase-space can be modulated in a way to allow for almost conventional TOF, selectable constant resolution from 3% to 20%, high-intensity specular reflectometry, etc. So it is possible to screen some parameters within a short time, and then to perform high-quality measurements with optimised conditions. Or to perform time-resolved investigations on the second-range.

The small footprints set high limits for the quality of the guides and the possibility to align them. Since the focal spot size is given solely by the initial slit size, the de-tuning of the two guides (sections ?? and ??) and the surface fidelity of the guide, there is no possibility to reduce the beam spot with slits after the end of the guide system.

Since for very small samples it will still be difficult to reach high  $q_z$  or large dynamic ranges, the option of a full-convergent beam geometry (??) is ideally suited for this application.

The need to reduce background and to increase radiation safety might lead to more shielding than given in the ESS baseline (6 m radius for the monolith), or as mentioned at IKON3 (12 m radius, no line of sight, no line of sight to directly irradiated area). Since the *Selene* guide systems implies an *early* manipulation of the beam, the geometrical situation and the accessibility of the *early* region of the beamline strongly affects the instrument lay-out. Thus the options and parameters given in the following sections can not be final, but they reflect the actual state of the work.

## 2.1 science case

Typical small samples are hard matter heterostructures where the production process limits the (homogeneous) area to below  $1\text{ cm}^2$ . This is e.g. the case for layered metal oxide films grown by pulsed laser deposition (PLD).

...

The need to reach high  $q_z$  and thus high detector angles (up to  $46^\circ$  for  $q_z = 1\text{ \AA}^{-1}$ ,  $106^\circ$  for  $q_z = 2\text{ \AA}^{-1}$ ) favours a horizontal scattering geometry. This is also supported by the fact that than gravity affects the beam profile and divergence only in the sample plane.

The only restriction caused by the vertical sample plane is that liquid/gas and liquid/liquid interfaces can not be studied.

### **magnetic metallic or oxidic heterostructures**

This group of materials are the main target for the small samples reflectometer. Depending on the materials involved the samples are grown by pulsed laser deposition (PLD), sputtering, molecular beam epitaxy (MBE), or the like. Especially PLD-grown samples often suffer from the inhomogeneous thickness of the film for areas larger than  $5 \times 5\text{ mm}^2$ . The homogeneity is important not only for the reflectometry measurements, but also it often determines the properties of the film. E.g. the sign of magnetic coupling through a non-magnetic spacer layer might change as a function of the spacers thickness.

A widely used substrate for perovskite-type heterostructure is  $\text{SrTiO}_3$ , which upon cooling undergoes several phase transitions. The one at 105 K leads to a twinning and as a consequence to a fragmentation of the surface, where the individual facets reflect in different directions. With a small footprint one can reduce the number of active facets for measurements.

Samples investigated with synchrotron radiation methods often are below  $1\text{ cm}^2$  to fit in the HV sample environment. The presented instrument would be able to investigate the same samples for complementary information. E.g. in combination with XRD, XMCD and resonant x-ray reflectometry.

Samples showing eclectic effects (polarisation, multiferroic properties) often need to be conducted. A focused beam then allows to measure in a region without contacts to avoid uncontrolled absorption, background and eventually phase shifts in part of the reflected neutrons (e.g. contact/film interface instead of vacuum/film).

### **non-magnetic metallic or oxidic heterostructures**

#### **soft matter films and heterostructures on a substrate**

Since samples of this type often can be produced with surface area of  $10\text{ cm}^2$  to  $100\text{ cm}^2$  they would profit from a footprint width larger than  $\approx 1\text{ cm}$ . Nevertheless they can be investigated on this instrument.

... rare substances ....

... expensive material ....

### **liquid/solid interfaces**

Liquid/solid cells can be mounted and measured without problem. Since the footprint can be defined exactly way before the sample it is possible to avoid the illumination of the gasket and the liquid vessel. Again, for larger cells the width of the footprint might be less than acceptable by the sample. On the other side one can even reduce the footprint to scan the interface for inhomogeneities (e.g. non-perfect coating or air bubbles).

### **laterally structured surfaces**

For these it is essential to measure the off-specular reflected signal. This is possible by using a slit directly after the guide (2.4 m or 4.5 m from the sample) which leads to an almost conventional TOF reflectometry set-up. "Almost" means that the beam is still convergent! The slit just defines the  $\theta$ -range, not the footprint size. Moving the slit between pulses allows to vary  $\theta$  without rocking the sample.

## **GISANS**

The focused beam in principle allows for focused GISANS experiments. The area detector has to be put in the focal plane, the sample as far away as possible, i.e. close to the end of the guide. Without sample the beam spot on the detector is defined by the initial slit, its divergence by the guide, eventually reduced to fit the sample size.

A laterally structured sample, mounted in the convergent beam leads to scattering and diffraction.....

It is not yet clear if the beam leaving the guide is clean enough for high-quality GISANS measurements. Also the sample-detector distance of 2.4 m or 4.5 m is rather small and requires a high spacial resolution of the detector. On the other side one can use the full convergent beam, unlike when multy-channel collimators are used behind a guide with divergent beam.

### **spin-echo techniques**

In cooperation with Robert Georgii and Wolfgang Häußler, both from the Technical University Munich, we investigate the possibility to have a MIEZE set-up as an add-on. The second coil could be installed in the space before the sample, the first one in an equivalent position before the a guide element. This way all trajectories between the coils are of the same length.

The space before and behind the sample would also allow for the installation of a SERGIS set-up.

## 2.2 single-Selene guide system

The length and  $\lambda$ -range of the instrument is derived on basis of the argumentation given in (??) and (??). The horizontal divergence is defined by the fact that the first focal point must be outside the target monolith for the operation of beam-modulating devices. The vertical divergence is obtained by optimising the flux on the sample.

Within the beam extraction unit a first reflector is located. This helps to get out of the direct line of sight and it acts as a  $\lambda$ -filter. Outside the monolith a second, exchangeable reflector is positioned, which selects the operation modes (non-) polarised, high-intensity specular reflectometry, and  $\lambda$ - $\theta$ -encoding with variable resolution. Behind this a precision slit system defines the footprint and forms the initial focal point of the *Selene* guide system, which extends to the sample. Figure 12 shows a possible layout and measures for this instrument, tables 2 and 3 contain the parameters of the instrument and the guide.

Within the guide, each neutron undergoes exactly 4 reflections, leading to moderate losses due to the finite reflectivity, only. But the shielding of the guide is challenging: there is direct view from the end of the second guide element to the entrance of the first one, so that there is not much space for shielding in addition to the monolith.

Table 2: Physical parameters and properties of the reflectometer for small samples using a single *Selene*-type guide.

parameter space		
$q_z$ -range	$[0, 1] \text{ \AA}^{-1}$	to be covered in 5 measurements
$\lambda$ -range	$[5, 9.3] \text{ \AA}$	
sample size	$[0.3, 10] \times [0.3, 10] \text{ mm}^2$	
maximum divergence	$\Delta\theta_{xy} = 1.0^\circ$ $\Delta\theta_{xz} = 2.0^\circ$	scattering plane sample plane
resolution		
$\Delta q/q = \text{constant}$	3%, 5%, 10%, ...	with multilayer monochromator
$\tau = \text{constant}$		no pulse shaping
moderator	cold	
geometry		
scattering plane	horizontal	
total length	58.0 m	
moderator / end of shielding	26.0 m	
end of guide / sample	4.5 m	
sample / detector	6.2 m	
$2\theta$	$-2^\circ$ to $50^\circ$ ( $110^\circ$ )	for $q_z \leq 1 \text{ \AA}^{-1}$ ( $2 \text{ \AA}^{-1}$ )
detector		
angular width	$4^\circ \times 8^\circ$	vertical $\times$ horizontal
angular resolution		
size	$420 \times 840 \text{ mm}^2$	for 6.2 m distance to sample
pixel size	$1 \times 1 \text{ mm}^2$	"
options		
polarisation & analysis		
sample environment	cryo-magnet	
add-on	MIEZE, SERGIS	

Table 3: Parameters of the *Selene*-type guide. For a given instrument length of 58 m and  $\Delta\theta_{xy} = \Delta\theta_{xz} = 1.5^\circ$  the following guide parameters are obtained by analytical calculations. For the beam extraction see also (??).

guide parameters		
$c$	11.25 m	
$\xi$	0.6	
$b/a$	0.01173	horizontal
	0.02335	vertical
coating	$m = 1.7$	horizontal
	$m = 3.4$	vertical
distances		
moderator / focal plane	6.4 m	first focal point
$2c$	22.5 m	length of ellipses
$\xi \cdot 2c$	13.5 m	length of (coated) guide sections
$(1 - \xi) \cdot 2c$	9.0 m	space between guides
$(1 - \xi) \cdot c$	4.5 m	space before sample
sample / detector	[1.5 ... 7.5] m	high-angle diffraction vs. high resolution
free space for chopper locations (distance from the moderator)		
	6.0 m → 10.9 m	
	22.4 m → 33.4 m	
	46.9 m → 51.4 m	
transmission		analytical, based on eqn. ??
$\lambda$	$t$	
5 Å	58%	
6 Å	68%	
7 Å	76%	
8 Å	82%	
9 Å	86%	
$q_z$ ranges for one angular setting		
$\theta_{\min}$	$q_z$ range	
0.4°	0.01 Å <sup>-1</sup> → 0.06 Å <sup>-1</sup>	
2.5°	0.06 Å <sup>-1</sup> → 0.15 Å <sup>-1</sup>	
6.0°	0.14 Å <sup>-1</sup> → 0.30 Å <sup>-1</sup>	
13.0°	0.30 Å <sup>-1</sup> → 0.60 Å <sup>-1</sup>	
26.0°	0.58 Å <sup>-1</sup> → 1.14 Å <sup>-1</sup>	

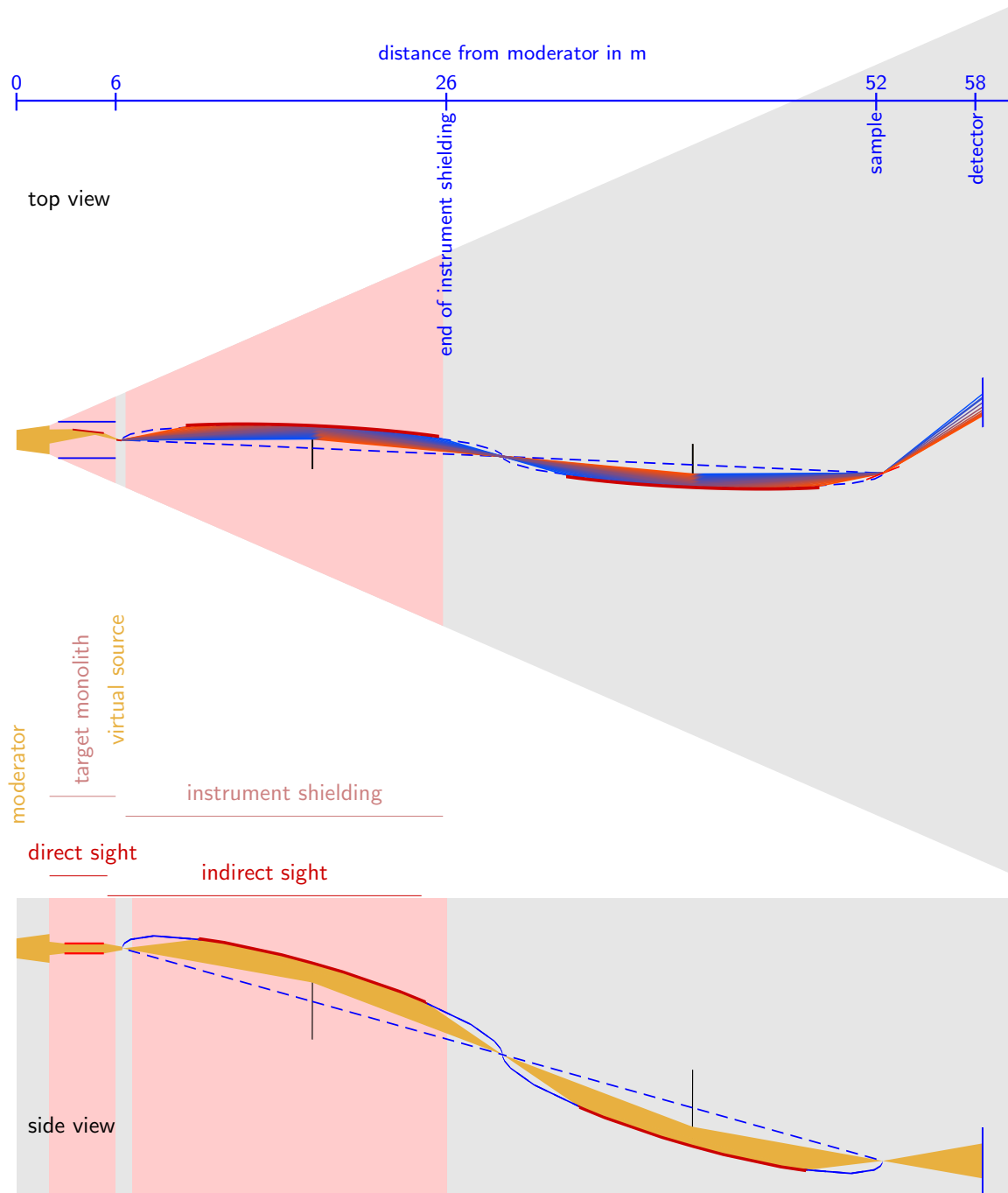


Figure 12: Schematic vertical and horizontal layout of the reflectometer with a horizontal scattering geometry, and with the first slit ( $P_1$ ) outside the target monolith. The gray wedge corresponds to a  $5^\circ$  segment, the light red areas are the biological and the instrument shielding. The parameters used for these sketches are  $a_{xy} = a_{xz} = 8000$  mm,  $b_{xy}/a_{xy} = 0.02$ ,  $\Delta\theta_{xy} = 2^\circ$ ,  $b_{xz}/a_{xz} = 0.011$ , and  $\Delta\theta_{xz} = 1.1^\circ$ . The beam extraction lay out is the one discussed in section ??.

## simulations

Based on the parameters given in the previous section an instrument file for McStas was developed (T. Panzner) and a series of simulations were performed. Essentially these are:

- $\lambda$ - $\theta$  encoding by using a ML monochromator after the beam extraction.
- High-intensity specular reflectometry by substituting the ML monochromator by a supermirror.
- Almost conventional reflectometry by using a slit to cut down the divergence given by the set-up (b).

Figure 13 shows sketches the operation modes and the corresponding  $I(\lambda, \theta)$  maps as detected with a 1000 Å Ni film on Si as a sample. The sample size was  $5 \times 5 \text{ mm}^2$ .

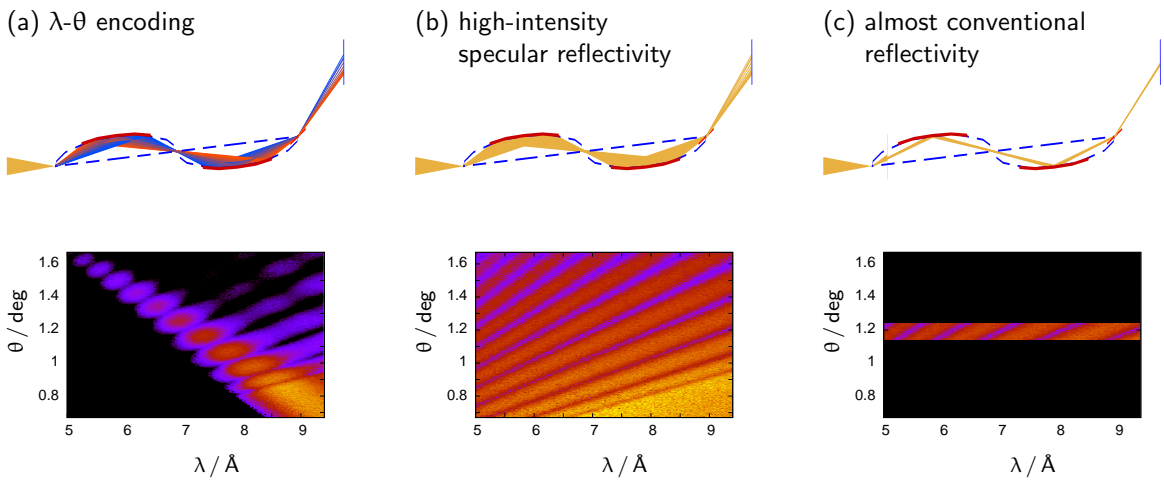


Figure 13: Operation schemes and  $I(\theta, \lambda)$  maps obtained by simulation assuming a 1000 Å thick Ni film on glass as sample: (a) using a multilayer monochromator for angle-wavelength encoding (in 60 s), (b) using full divergence and pulse (in 1 s), and (c) using a slit before the sample (in 10 s).

Form these maps the reflectivity curves shown in figure 14 were obtained by integrating over  $q_z$ . For accuracy measurement times of 60 s, 1 s, and 10 s were taken to get approximately the same statistical errors.

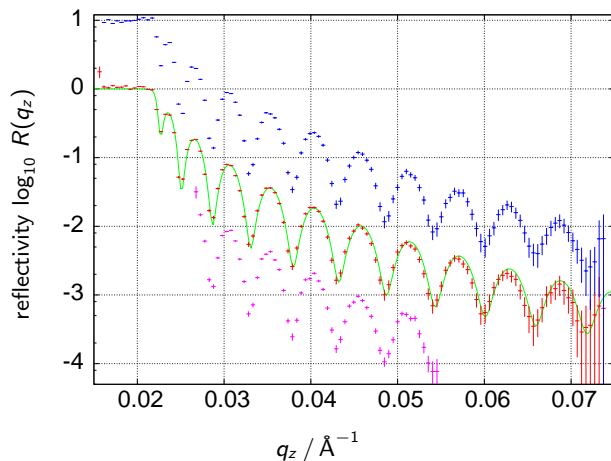


Figure 14: Reflectivities  $R(q_z)$  extracted from the maps shown in figure 13 (and scaled by 10, 1 0.1 for clarity). The green line corresponds to the initial reflectivity with  $\Delta q/q = 2.4\%$ . The covered  $q_z$  range and the resolution functions depend on the measurement scheme.

## 2.3 double-Selene guide system

This is an alternative approach to the one discussed above (2.2), paying respect to much higher shielding demands. If the target monolith and the shielding around the first guide are not sufficient (as is claimed by the experts from ISIS and SNS), one can build a guide system with 2 subsequent *Selene* sections. The first looks on a fix pin hole in the extraction section and creates a small but homogeneous virtual source some 20 m to 30 m from the moderator. From there direct and first indirect line of sight is blocked efficiently. The beam is then manipulated (shaped, polarised, filtered) at or close to that virtual source point and fed into the second *Selene* guide system.

The considerations for the instrument length are the same as in (2.2), but the divergences can be chosen more flexibly since the aperture defining the virtual source at the first focal point does not need to be manipulated and can be located anywhere in the target monolith (after 2 m from the moderator). Tables 4 and 5 give the parameters of the instrument and guide, and figure 15 shows a possible realisation.

Table 4: Physical parameters and properties of the reflectometer for small samples using two subsequent *Selene*-type guides.

parameter space		
$q_z$ -range	$[0, 1] \text{ \AA}^{-1}$	to be covered in 5 measurements
$\lambda$ -range	$[5, 9.3] \text{ \AA}$	
sample size	$[0.3, 10] \times [0.3, 10] \text{ mm}^2$	
maximum divergence	$\Delta\theta_{xy} = 1.5^\circ$ $\Delta\theta_{xz} = 1.5^\circ$	scattering plane sample plane
resolution		
$\Delta q/q = \text{constant}$	3%, 5%, 10%, ...	with multilayer monochromator
$\tau = \text{constant}$		no pulse shaping
moderator	cold	
geometry		
scattering plane	horizontal	
total length	58.0 m	
moderator / end of shielding	26.0 m	
end of guide / sample	2.4 m	
sample / detector	6.2 m	
$2\theta$	$-2^\circ$ to $50^\circ$ ( $110^\circ$ )	for $q_z \leq 1 \text{ \AA}^{-1}$ ( $2 \text{ \AA}^{-1}$ )
detector		
angular width	$4^\circ \times 8^\circ$	vertical $\times$ horizontal
angular resolution		
size	$420 \times 840 \text{ mm}^2$	for 6.2 m distance to sample
pixel size	$1 \times 1 \text{ mm}^2$	"
options		
polarisation & analysis		
sample environment	cryo-magnet	
add-on	MIEZE, SERGIS	

Using two *Selene* sections has the result, that the guide dimensions are reduced by a factor 2, gravity effects are reduced by a factor 4, but the number of reflections in the guide increases from 4 to 8. This means that this approach favours longer wavelengths where the reflectivity of the coating is more efficient.

Table 5: Parameters of the *Selene*-type guide. For a given instrument length of 58 m and  $\Delta\theta_{xy} = \Delta\theta_{xz} = 1.5^\circ$  the following guide parameters are obtained by analytical calculations. For the beam extraction see also (??).

guide parameters		
$c$		6.0 m
$\xi$		0.6
$b/a$		0.01754
coating		$m = 2.5$
distances		
moderator / pin hole	4.2 m	first focal point
$2c$	12.0 m	length of ellipses
$\xi \cdot 2c$	7.2 m	length of (coated) guide sections
$(1 - \xi) \cdot 2c$	4.8 m	space between guides
$(1 - \xi) \cdot c$	2.4 m	space before sample
sample / detector	[1.5 ... 7.5] m	high-angle diffraction vs. high resolution
free space for chopper locations (distance from the moderator)		
	6.0 m → 6.6 m	
	13.8 m → 18.6 m	
	25.8 m → 30.6 m	
	37.8 m → 42.6 m	
transmission		analytical, based on eqn. ??
$\lambda$	$t$	
5 Å	34%	
6 Å	47%	
7 Å	58%	
8 Å	68%	
9 Å	77%	

$\lambda$	$t$
5 Å	34%
7 Å	58%
9 Å	77%

$q_z$  ranges for one angular setting

$\theta_{\min}$	$q_z$ range
$0.4^\circ$	$0.01 \text{ \AA}^{-1} \rightarrow 0.08 \text{ \AA}^{-1}$
$3.0^\circ$	$0.07 \text{ \AA}^{-1} \rightarrow 0.19 \text{ \AA}^{-1}$
$7.7^\circ$	$0.18 \text{ \AA}^{-1} \rightarrow 0.38 \text{ \AA}^{-1}$
$16.0^\circ$	$0.37 \text{ \AA}^{-1} \rightarrow 0.72 \text{ \AA}^{-1}$

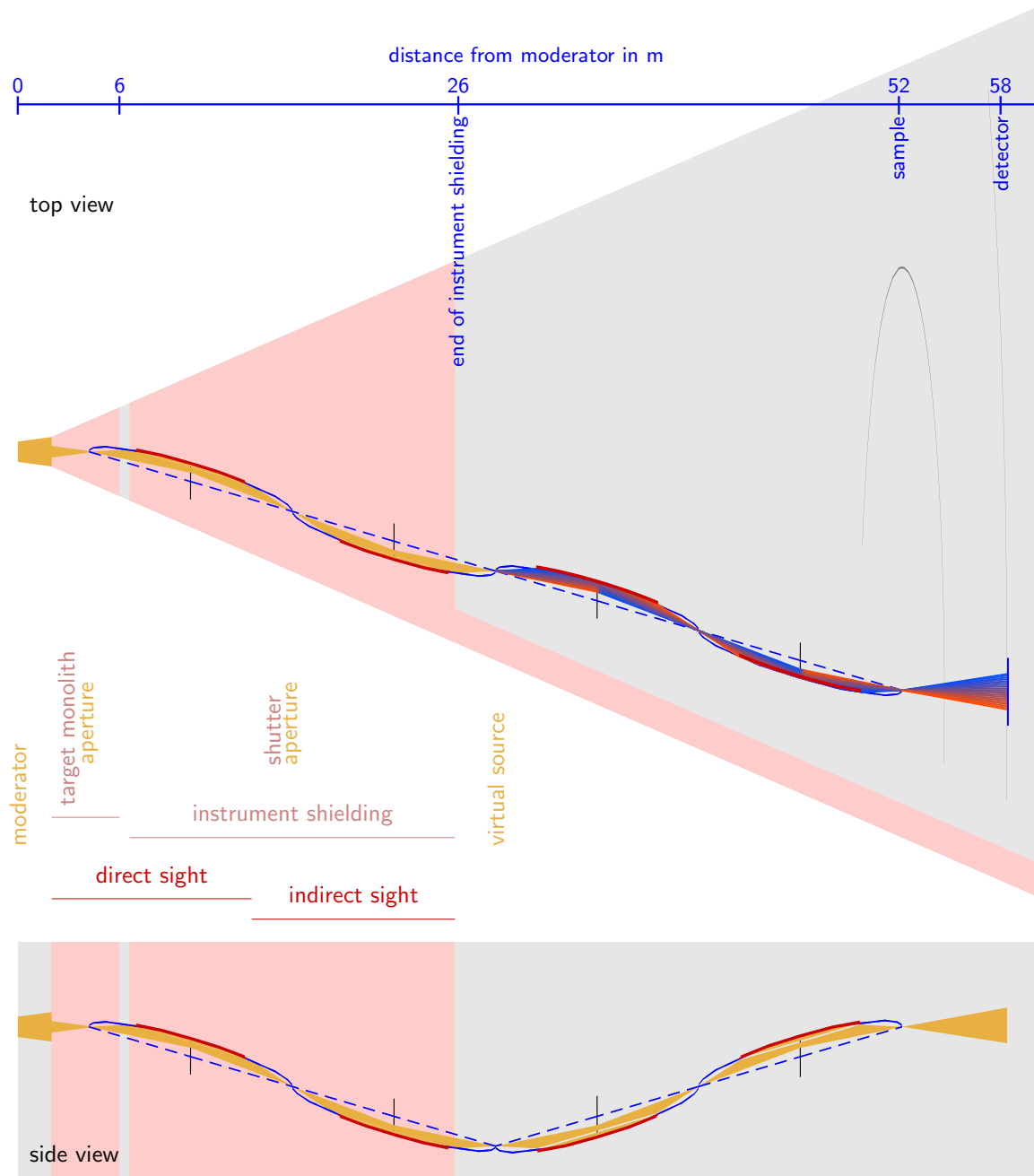


Figure 15: Sketch of a guide system with two subsequent pairs of ellipses. A small ( $10 \times 10 \text{ mm}^2$ ) aperture 4.2 m from the source acts as the initial focal slit for the first *Selene* guides. These are completely within a shielding. Direct line of sight to the source is possible all along the first guide element. Secondary radiation can be directly seen all along the second guide element. Behind that the beam is focused down to the size of the initial aperture. At that point the precision shaping of the footprint is performed. The second *Selene* guide acts as in the set-up described above. This way the shielding ends some 26 m after the moderator. The beam channel is bent several times so that the radiation level should be much reduced. The polariser or a band-pass filter will be positioned in a low-radiation region easily accessible for maintenance.

## 3 reflectometer with a horizontal sample surface

The potentially horizontal surface of the sample allows for measurements of liquid/gas or liquid/liquid interfaces. Typically these samples are larger than  $10 \times 10 \text{ mm}^2$ , so that the requirements for focusing are relaxed. This is important for the chromatic aberration in the scattering plane introduced by gravity.

The high incoherent background to be expected from these samples, especially for a full converging beam, or multibeam set-up limits the simultaneous usability of the full beam. But using a technique to disentangle  $\lambda$  and  $\theta$  as proposed in sections ?? and ?? allows to reach a wider  $q_z$ -range without touching the sample or the instrument geometry, except for a slit-position or a chopper phase.

### 3.1 science case

(from the draft for the 2012 contract with the ESS, by B. Klösgen)

The high flux of the ESS combined with this focusing concept will enable fast data acquisition (sec or less) thus allowing for reduced sample areas (or subphase), scanning of large sample sets, or the acquisition of time correlated reflectivity data. The instrument is optimised for measuring on free-standing liquids and horizontally oriented thin films and interfaces. It will provide coverage of a wide  $q$ -range ( $0.006 \text{ \AA}^{-1}$  to  $0.30 \text{ \AA}^{-1}$ ) at low background, providing a reflectivity range down to  $10^{-7}$  to  $10^{-8}$  as it must be requested for the study of molecularly thin films. This is achieved with one to two incident angles only, with exposure times in the range of fractions of seconds. The scientific case includes structural characterization of (liquid) interfaces and thin films, both soft and hard matter, the probing of rearrangement dynamics within the film and at interfaces, and the potential use of as a density profilometer type reflectometer. Examples are structural studies of molecular films (monolayers, bi-layers, and oligo-layers) such as (bio-)membranes or surfactant mesostructures at the liquid-gas / liquid-liquid interface or liquid-solid supported thin films. The instrument will comprise the option of polarisation and polarisation analysis, e.g. for magnetic studies, contrast enhancement, or possibly a spin-echo upgrade. It will allow for sample environment as Langmuir trough equipment, Brewster angle microscopy, or IR spectroscopy. The goal is to provide a versatile tool for expanding research topics as exotic biological or biomimetic materials, future composite functional materials or the application of expensive deuterated compounds.

### 3.2 instrument

#### 3.2.1 operation principle

(by U. Hansen)

The *Selene* guide just leads to an parallel shift of the beam so that the down (up) bending has to be realised before the *Selene* guide section (in or directly after the beam extraction). This inclination together with  $\Delta\theta$  defines the possible angles of incidence on a liquid sample in the *first setting*.

#### reflector at intermediate focal point

To access higher angles and thus higher  $q_z$  one (or several) reflecting mirrors have to be used at the intermediate focal point and eventually the top branch of the second ellipse is needed (*second setting*). Figure 16 shows the two possible modes of the *Selene* concept. The mirror in between the two guides has to be tilted to reach a specific angular range. As a consequence also the second ellipse is rotated and the sample position moves.

The mirror in between the two ellipses introduces an extra rotation of the beam profile and the entrance slit position should be modified accordingly so the beamprofile is still horizontal at the sample position.

The available space limits the length of the mirror and thus the angular range where it can be operated. In addition the  $m$  value of the coating sets some restrictions.

Table 6: Physical parameters and properties of the reflectometer for horizontal sample surfaces.

parameter space		
$q_z$ -range	$[0.006, 0.3] \text{ \AA}^{-1}$	to be covered in 5 measurements
$\lambda$ -range	$[3, 11] \text{ \AA}$	
sample size	$[1, 10] \times [10, 50] \text{ mm}^2$	
maximum divergence	$\Delta\theta_{xy} = 2.5^\circ$ $\Delta\theta_{xz} = 2.5^\circ$	scattering plane sample plane
resolution		
$\Delta q/q = \text{constant}$	3.3% – 11.3%	
moderator		
cold		
geometry		
scattering plane	vertical	
total length	30.0 m	
moderator / end of shielding	15.0 m	
end of guide / sample	1.8 m	
sample / detector	1.5 ... 3.5 m	
$2\theta$	$0.6^\circ$ to $2.8^\circ$	1st setting for liquid surface
	$2.8^\circ$ to $7.9^\circ$	2nd setting for liquid surface
sample size	$15 \times 50 \text{ mm}^2$	for precise footprint definition
options		
polarisation & analysis		
sample environment	Langmuir trough Brewster angle microscope IR spectrometer	

Table 7: Parameters of the *Selene*-type guide. For a given instrument length of 30 m and  $\Delta\theta_{xy} = \Delta\theta_{xz} = 2.5^\circ$  the following guide parameters are obtained by analytical calculations.

guide parameters		
$c$	5 m	
$\xi$	0.6	
$b/a$	0.02679	horizontal
	0.02679	vertical
coating	$m = 7.0$	horizontal
	$m = 7.0$	vertical
distances		
moderator / focal plane	6.5 m	first focal point
$2c$	10.0 m	length of ellipses
$\xi \cdot 2c$	6.3 m	length of (coated) guide sections
$(1 - \xi) \cdot 2c$	3.7 m	space between guides
$(1 - \xi) \cdot c$	1.8 m	space before sample
sample / detector	$[1.5 \dots 3.5] \text{ m}$	
free space for chopper locations (distance from the moderator)		
	6.0 m → 8.3 m	
	14.7 m → 18.3 m	
	24.7 m → 26.5 m	
$q_z$ ranges for one angular setting		
$\theta_{\min}$	$q_z$ range	
$0.3^\circ$	$0.006 \text{ \AA}^{-1} \rightarrow 0.205 \text{ \AA}^{-1}$	
$1.4^\circ$	$0.028 \text{ \AA}^{-1} \rightarrow 0.285 \text{ \AA}^{-1}$	

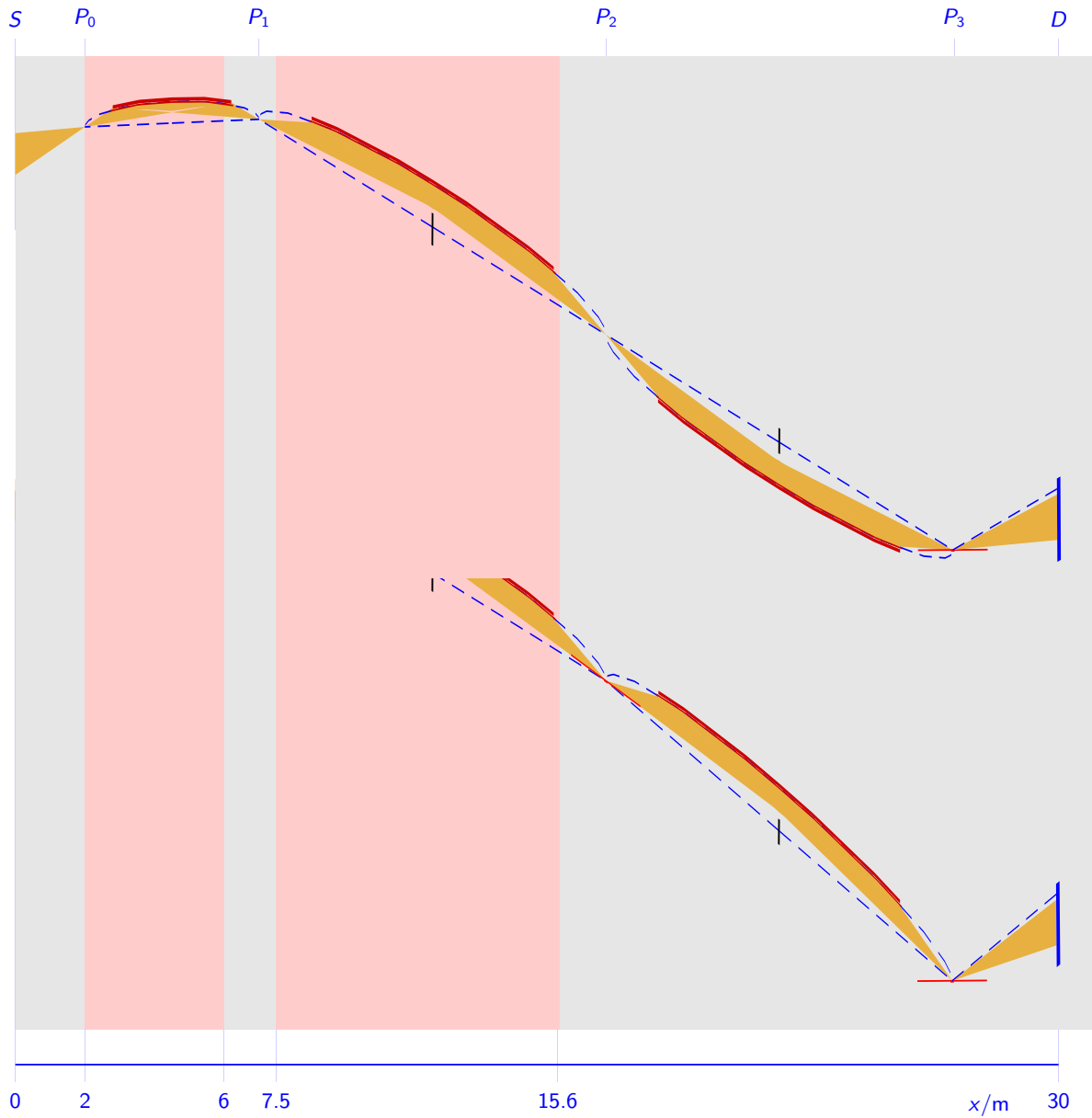


Figure 16: Schematic vertical lay-out of the reflectometer with a vertical scattering geometry, and with the first slit ( $P_1$ ) outside the biological shielding. The light red areas are the biological and the instrument shielding. The vertical axis is stretched by 10. *Top*: Standard setting to cover  $0.005 \text{ \AA}^{-1} < q_z < 0.23 \text{ \AA}^{-1}$ . The height difference between source and  $P_1$  is = 168 mm, and between source and  $P_3$  one gets  $-539$  mm. *Bottom*: High- $q_z$  setting using a reflector at  $P_2$  and the upper branch of  $E_2$ . Here the difference between source and  $P_3$  of  $-679$  mm. The parameters were chosen in a way that the beam divergence is symmetric to the horizont at  $P_2$ .

### footprint-defining diaphragm

The initial slit placed at the first focal point of the Selene ellipses, defines the beam footprint on the sample. Instead of a conventional slit system, the idea is to use a horizontal slit system where the length and width of the footprint on the sample is defined directly, see figure 17.

This approach makes use of the imaging properties of the *Selene* guide: a 3-dimensional object at the initial focal point is mapped to an image object at the final focal point. A slit system defining a *glowing area* (by cutting away everything outside) can produce a sharp footprint on a sample surface.

Figure 17: to come: sketch of the footprint-defining slit system.

### 3.2.2 McStas simulations

The intensity maps in figure 18 show the extend of the footprint on the sample surface in both directions and for both settings. These result from the neutron ray-trace simulation package McStas. The simulated *Selene* guides are built on the component `Guide_four_side.comp` written by Tobias Panzner. Gravity is so far not included in the simulations. The optimizations of the simulated instrument are conducted within the iFit Data Analysis library written by E. Farhi.

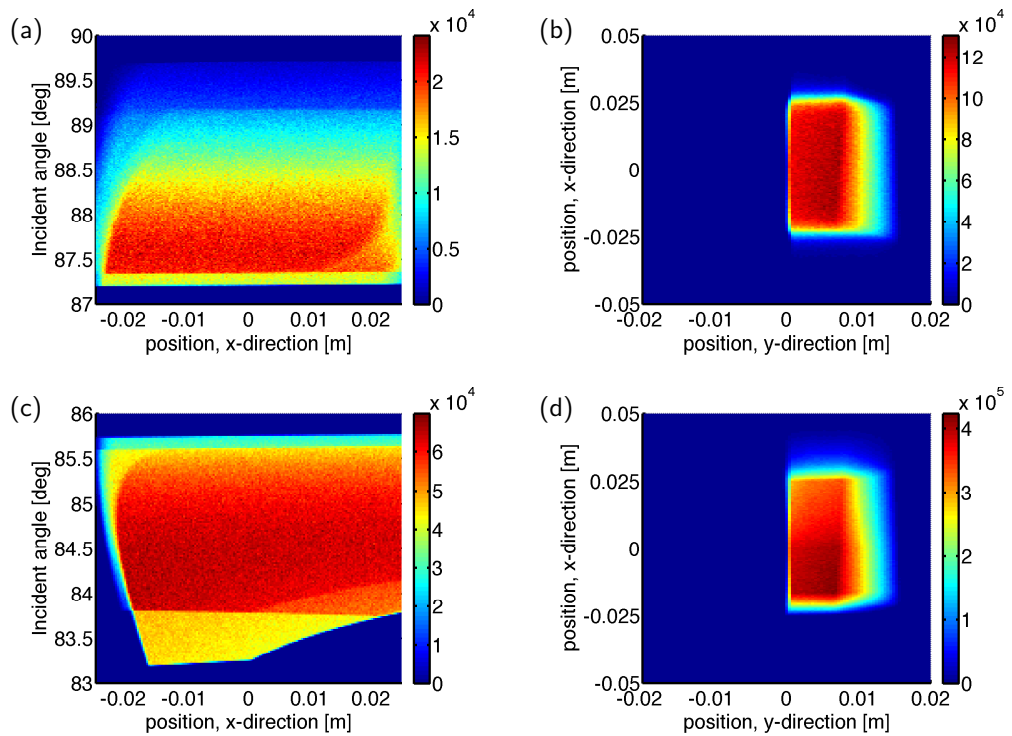


Figure 18: Intensity maps for  $I(x, \theta_{xz})$  (left, along the beam direction) and  $I(y, \theta_{xy})$  (right, normal to the beam) at the sample surface. (a) and (b) are obtained in the first setting, i.e. without mirror at the intermediate focal point, (c) and (d) in the second setting, with a mirror and after readjusting the initial slit.

## A publications

The *Selene* concept and experimental results were published as refereed manuscripts, as oral presentations and on posters. The following table chronologically lists publications and reports connected to this work.<sup>1</sup>

### reviewed publications

- 2012 *Focusing specular neutron reflectometry for small samples*  
J. Stahn, U. Filges, T. Panzner  
European Physical Journal - Applied Physics **58**, 11001 (2012)  
DOI:10.1051/epjap/2012110295
- 2011 *Neutron reflectometry by refractive encoding*  
R. Cubitt, J. Stahn  
Eur. Phys. J. Plus **126**, 111 (2011)  
DOI:10.1140/epjp/i2011-11111-0
- *Study on a focusing, low-background neutron delivery system*  
J. Stahn, T. Panzner, U. Filges, C. Marcelot, P. Böni  
Nuclear Instruments and Methods A **634**, S12 (2011)  
DOI:10.1016/j.nima.2010.06.221
- 2009 *Focusing of cold neutrons*  
— *performance of a laterally graded and parabolically bent multilayer*  
M. Schneider, J. Stahn, P. Böni  
N.I.M. A **610**, 530-533 (2009)  
DOI:10.1016/j.nima.2009.08.047

### oral presentations

- 2012/07 *Selene — a focusing guide system*  
J. Stahn, et al.  
Institut Laue-Langevin, workshop on Neutron Delivery Systems  
9. - 11. July 2012 Grenoble, France
- 04 *progress report of the Swiss-Danish instrument initiative for the ESS*  
J. Stahn  
IKON 3, 18. - 19.04.2012, Berlin, Germany
- 04 *Selene*  
J. Stahn  
ESS workshop on elliptic neutron guides, 17. 4. 2012, Berlin, Germany
- 03 *concept for a reflectometer using focusing guides*  
J. Stahn, T. Panzner, U. Filges  
TUM & FRM II seminar, 12.03.2012, München, Germany
- 02 *progress report of the Swiss-Danish instrument initiative for the ESS*  
*WP2: focusing reflectometer*  
J. Stahn  
IKON 2, 09. - 10.02.2012, Malmoe, Sweden
- 01 *Concept for a reflectometer for the ESS with focusing in the sample plane and in the scattering plane*  
J. Stahn, U. Filges, T. Panzner  
Workshop on off-specular neutron scattering, 09.-10.01.2012, Bruxelles, Belgium

---

<sup>1</sup>The presentations are linked or deposited for download on the web-page  
<http://people.web.psi.ch/stahn/publications.html>.

- 2011/10 *TOF reflectometry at PSI: from an optical bench set-up to a new instrument concept with a focus on small samples*  
J. Stahn  
JCNS instrumentation workshop, 04. -07. 10. 2011, Tutzing, Germany
- 09 *concept for a reflectometer for the ESS with focusing in the sample plane, and a convergent beam in the scattering plane*  
Jochen Stahn  
meeting of the ESS reflectometry TAP, 15. 09. 2011, Lund
- 09 *concept, design and first results: convergent-beam reflectometry using a focusing elliptic guide*  
Jochen Stahn, Uwe Filges, Tobias Panzner, Martie Cardenas, Beate Klösgen  
IKON-1, First In-Kind Contributions Meeting for Neutron Science for the ESS  
8. 9. 2011, Lund, Sweden
- 07 *Selene: high-intensity specular reflectometry*  
J. Stahn, U. Filges, T. Panzner  
5th European Conference on Neutron Scattering, ECNS 2011  
July 17.-22. 2011, Prague, Czech Republic
- 2010/06 *specular reflectometry on small samples using a convergent beam*  
J. Stahn  
reflectometer seminar, Oslo, 17. 06. 2010
- 05 *study on a focusing, low-background neutron delivery system*  
J. Stahn, T. Panzner, U. Filges  
JCNS seminar, Garching, 04. 05. 2010
- 03 *study on a focusing, low-background neutron delivery system*  
J. Stahn, T. Panzner, U. Filges  
neutron optics workshop NOP2010, Alpe d'Huez, 17.-19. 03. 2010
- 2008/06 *elliptic neutron guides - from the idea to the implementation*  
J. Stahn  
nmi3 meeting 2008, Corse, France: JRA3 - Neutron Optics
- 06 *laterally graded and complex multilayers for neutron optical elements*  
J. Stahn  
nmi3 meeting 2008, Corse, France: JRA3 - Neutron Optics
- 04 *elliptic beam guide - concept and first tests*  
J. Stahn  
ILL workshop on neutron guides, 26., 27. 04. 2006, ILL, Grenoble
- poster**
- 2012/04 *Science and Scientists @ ESS - conference: 19th-20th of April, 2012, Berlin, Germany:*  
*Selene-type reflectometer — principle*  
*Selene-type reflectometer for small samples*  
*Selene-type reflectometer — prototype on BOA*  
J. Stahn, T. Panzner, U. Filges, M. Cardenas, B. Klösgen, U. Bengaard Hansen